2022

Plasmonic Sensor Based Detection of Dopamine

Sang Lee
University of Central Florida

PLASMONIC SENSOR BASED DETECTION OF DOPAMINE

By

SANG JUN LEE
B.S. University of Central Florida, 2016

A thesis submitted in partial fulfillment of the requirements
for the degree of Master of Science
in the NanoScience Technology Center
in the College of Graduate Studies
at the University of Central Florida
Orlando, Florida

Fall Term
2022

Major Professor: Debashis Chanda

ABSTRACT

With a rapidly ageing population, neurological diseases are becoming increasingly relevant in the design of public health policies and strategies in western societies. In the last decades, biochemical research has consistently shown the critical role that neurotransmitters and their associated metabolites play as biomarkers in tracking and diagnosis of different brain disorders and cancers. In particular, dopamine, an organic electrochemical neurotransmitter, has been shown to be paramount for the proper functioning of the neural system. Dopamine's dysfunction, has been shown to underlie the pathogenesis in several neurological disorders such as Parkinson's disease, depression, chronic schizophrenia and psychosis. Unfortunately, currently available diagnostic technologies require expensive equipment and trained personnel, thus slowing the process and increasing overall costs, consequently reducing the access to the general population. Ideal sensing alternatives should offer low-cost, fast, and reliable point-of-care diagnosis. In this work, we present a compact label-free plasmonic biosensors that exhibits sharp optical resonance shifts in response to varying dopamine concentrations. While the nanoimprinting of the optical cavity offers a nanofabrication process fully compatible with large-scale production, its small size ensures the suitability for

integration on lab-on-a-chip platforms, hence making it a promising alternative to conventional diagnosis. The plasmonic nanostructures of the chips are functionalized with synthetic single-stranded oligonucleotide to ensure precise sensing selectivity. Particularly, we study the standard 57mer and the novel 44mer configurations, establishing the superior resolution offered by the latter. In contrast to other sensing alternatives, our platforms permit reliable detection with ultralow volumes (~6 μL) and exhibit robustness to interfering species. This work paves the way towards the first generation of low-cost, ultra-low volume, on-chip sensors for in-situ tracking of dopamine.

ACKNOWLEDGEMENTS

I would like to personally thank Dr. Debashis Chanda who personally gave me a wonderful opportunity to work in a field I'm passionate about and aided me throughout my journey. Furthermore, I would like to thank my fellow colleagues who have helped me tribulations such as Aritra Biswas, Dr. Pablo Cencillo, Bryan Pamela, Waqas, Jared, Sayan, Francisco. They have looked after my wellbeing and worked in conjunction with me to ensure that I would graduate. Furthermore, I would like to thank my family who allowed and supported my dreams to pursue this field. I would also like thank committee members Dr. Kiminobu Sugaya, Dr. Ellen Kang, and Dr. Sudipta Seal for guidance and patience.

TABLE OF CONTENTS

LIST OF FIGURES

LIST OF ACRONYMNS AND ABBREVIATIONS

ADHD	Attention-deficit/hyperactivity disorder
AFM	Atomic Force Microscopy
ALD	Atomic Layer Deposition
AuNP	Au Nanoparticles
CNS	Central Nervous System
CSF	Cerebral Spinal Fluid
CV	Cyclic Voltammetry
DA	Dopamine
DPV	Differential Pulse Voltammetry
ECF	Extracellular Fluid
ELISA	Enzyme-Linked Immunosorbent assay
EPI	Epinephrine
FSCV	Fast-Scan Cyclic Voltammetry
HVA	Homovanillic Acid

L-Dopa	Levodopa
LSPR	Localized Surface Plasmon Resonance
MCH	6-Mercapto-hexanol
MSA	Multiple System Atrophy
PD	Parkinson’s Disease
PDMS	Poly Dimethyl Siloxane
PET	Positron Emission Tomography
PVA	Polyvinyl Alcohol
RMS	Root Mean Square
S.D.	Standard Deviation
SNIL	Soft Nanoimprint lithography
SPECT	Single Photon Emission Computed Tomography
TI	Titanium
UV	Ultraviolet

CHAPTER ONE: INTRODUCTION

1.1 Motivation

With the aging population growing dramatically due to better healthcare and living conditions, it has come to highlight other diseases that are more prevalent in the aging population. Neurological diseases such as Parkinson's, Alzheimer's, and dementia. Such diseases have created greater cost of burden in mental and physical aspects to society due to requiring caretakers for supervision and lowering quality of life standards thus cost health insurance significant amount of money (Pagano, 2016). Research creating a functionalized sensing platform to help detect signs of neurological diseases via low-cost, point of care system is relevant in the aging population.

1.2 Biomedical

Dopamine is defined as one a major neurotransmitter, which is a chemical messenger when released by stimulated neurons it communicates within the synapses. However, it is also known to be a neuromodulator meaning it can flow through fluids between the neurons and in return it affects diverse group of neurons or other the respective receptors. The mechanism of action occurs through volume

transmission meaning it travels through fluids of the Extracellular Fluid in the Central Nervous system (ECF) and Cerebral Spinal Fluid (CSF)(Kjell Fuxe, 2013).It plays a key role in controlling the central nervous system function such as locomotion, memory processing, reward mechanism and selected high cognitive functions (Luisa Speranza, 2021; Allen PF Chen, 2021). Due to dopamine's role being connected to managerial role of the CNS and its dysregulation leading to neuropsychiatric diseases, it has been heavily investigated due to create preventative measures to detect on set neurological degenerative diseases like Parkinson's.

The average incidence for Parkinson's is 4.1 to 21 per 100,000 people in the U.S., and with this being genetically linked, it has been reported that at least 25 percent have family history of Parkinson's disease (Pagano, 2016). Currently, 2-3 percent of the aging population of 65 and above are diagnosed to have Parkinson's disease in the U.S., meaning that nearly 1 million people have this neurodegenerative disease and likely to grow to 1.2 million by 2030 (Pagano, 2016). This disease alone has cost health insurance 52 billion annually in the U.S. and projected to go upwards (Yang, 2020).

Symptoms of Parkinson's diseases has been reported to not being detectable only after 30-50 percent loss of nigral neurons and 80 percent of striatal dopamine content (Stossel, 2012). The earliest diagnosis or symptoms for Parkinson's disease

is not dopamine deficiency, but conditions that produce tremors or akinetic-ridgid syndrome (ie. Multiple system atrophy (MSA)). However, MSA is associated with loss of dopamine receptors and is one of the keys to determine the differences between the 2, which requires molecular imaging in positron emission tomography (PET) or single photon emission tomography (SPECT) (Stossel, 2012). Unfortunately, both procedures are not easily accessible nor cheap and requires trained personnel and expensive machinery to create specific isotopes.

Dopamine was discovered to be biomarkers in certain clinical rare instances for cancer/tumor is also a biomarker for certain tumors such as Pheochromocytomas due to Dopamine-beta-hydroxylase increasing dopamine secretion, where concentrations of dopamine in serum or urine is to distinguish the different types of pehochromocytomas (Dubois, 2005). Neuroblastoma likewise to pheocrhomocytomas involves dopamine-beta-hydroxylase, and its activity was proportional to the activity and growth of the tumor. When the tumor was treated there was a decrease of dopamine-beta-hydroxylase (Anagnoste, 1972). In addition, an instance in of a clinical case where retroperitoneal paragangliomas exclusively produces excessive amount of dopamine. (Yi, 2012)

Dopamine also plays an essential role in cardiovascular system, where if the patient has high levels of dopamine, it can indicate cardiotoxicity and lead to

increased heart rate and possible heart failure in worst case scenario (Buculo, 2019). This is quite the contrast to diseases tied to the CNS where low levels is synonymous to major cause of the neurological diseases. Dopamine acts as an adrenergic argonist to alpha and beta adrenoreceptors when there are high levels of plasma concentrations introduced (Ruffolo et al., 1984)

Furthermore, dopamine plays a role in regulating the intraocular pressure of the eye via ciliary blood flow and aqueous humor production. This is important for glaucoma, for it is an irreversible blindness that impacts 60 million people when the IOP is elevated thus cause retinal ganglion cell death (Busco, 2019). The key dopamine receptor that is responsible for the management of IOP is D3R, this was proven when the mice that was induced ocular hypotension was reversed (Busco, 2012).

1.3 Current Methods in Dopamine detection

Dopamine research detection is divided into two main types of detection methods or approach that research groups take to tackle dopamine binding. It is bio-sensing and electrochemical detection. Bio sensing has enzyme, antibody, aptamer, and molecularly imprinted based sensors. Electrochemical detection are divided into

three subcategories cyclic voltammetry (CV), Fast-scan cyclic voltammetry (FSCV), and differential pulse voltammetry (DPV). There is research done where biosensing and electrochemical detection is using aptamer as a primary source of attachment for electrochemical detection for dopamine (Nakatsu, 2018). Dopamine is one of the neurotransmitters that is under three categories, and dopamine is under the category electrochemically active compound including others such as norepinephrine, epinephrine alongside of most of their metabolites therefore it is understandable that electrochemical detection is applicable (Adams 1990).

CV is a technique that derives from using three-electrode system comprised of counter, reference, and working electrodes. The counter and working will have the current flowing when the chemical reaction take place, the reference will remain constant potential to the other electrodes. From this, a cyclic voltammogram will be generated with the position and redox peaks along with the amplitude. This is determined by the neurotransmitter's chemical stability and electron transfer rate (Banjeer, 2020).

FSCV is a current technique used presently that is derived from cyclic voltammetry, it is when a current is produced by sweeping the potential between two electrodes through a specific range tailored to dopamine's redox reaction. The peak that it produces can signify qualitative and quantitative measurement and can overcome ascorbic acid or other fluids that may tamper in other electrochemical reading such as amperometry (Lakard, 2020). FSCV can be performed real time due to its fast detection but requires an electrode that has fast capacitive charging while have a small-time constant (Wightman, 1981). The one that currently fits this criterion is carbon-nanotube modified microelectrodes and been functionalized to absorb cations via surface oxide functional groups (Huffman, 2008).

DPV is when the base potential value that does not contain any faradaic reaction but is also applied to the electrode. The same potential increases in equal increments between the pulses. Before each current change, the point is measured and the potential difference is plotted and measured against uninitiated current change's potential. In addition, charging current is avoided due to the immediate sampling of the current, furthermore when the analyte process begins the DPV technique creates a more accurate peak than linear is often paired with biosensors to differentiate analyte and surrounding solution or noise (Lakhard. 2021).

1.4 Plasmonic sensors

Traditional detection methods that use labeling to detect biomarkers or analytes are generally fall under enzyme-linked immunosorbent assay (ELISA), fluorescence, and western blot assay (Wild, 2007). The issue with these traditional methods is that it requires trained personnel, labor intensive, and time consuming where it may require specialized equipment to analyze the biomarker, which in itself may need large quantity or concentration of biomarker. An alternative bio-sensing detection method that this paper explores exploits the phenomenon of localized surface plasmons (LSP). When the light interacts with the nanoparticles the conduction electrons will oscillate together with a resonant frequency dependent on the same nanoparticle's composition, size and shape (Anker, 2008). It is stated that 80-nm silver nanoparticle in the 445-nm blue light is a million times brighter than fluorescein molecule in a florescence cross-section and thousand-fold brighter when compared to similar sized nanoparticles/sphere with fluorescein with the self-quenching limit (Shultz, 2000).

The majority of such LSP based biosensors are developed into periodic two-dimensional arrays of isolated nanoparticles or long metallic films with pierced holes (Vasquez, 2016). They are created with the following top-down techniques such as electron-beam lithography, focused-ion beam lithography, hole-mask colloidal

lithography, and or nanosphere lithography (Vasquez, 2016). Techniques such as electron-beam and focused-ion beam require expensive machine and is time consuming. In contrast, nanosphere and hole-mask colloidal lithography is cheaper to produce but harder to reproduce over large surface area (Nemiroski, 2014).

The plasmonic device that is used in this experiment consists of a top gold-based surface with circular holes and disks spatially separated in the vertical plane. This is coupled to a resonator cavity formed by a cured negative photosensitive resist on a gold mirror and is designed with soft nanoimprint lithography (SNIL) technique which in return produce high quality and reproducible biosensing substrates. The resonator mode coupled with the intrinsic local surface plasmons on the top hole-disk layer generates a hybrid plasmonic spectral response. In the visible domain, several higher order electric and magnetic modes are generated and are visualized as localized surface plasmon resonances (LSPR) with great quality (Q)-factor. Since the LSPR are a result of nearfield EM confined enhancement, they are extremely sensitive to local changes in the environment. This property can be exploited to perform sensitive detection of proteins, viral strains and biomolecules, subject to appropriate functionalization of the top surface (Vasquez 2016; Vasquez 2019). In addition, unlike other surface plasmonic sensors these sensors are designed to be reproducible in a large scale due to the SNIL technique that allows high spatial

resolution around 30 nm for most 2D and 3D sensors over large flat or curved surfaces without additional work. Furthermore, the developed nanoimprinted surfaces with locked-in dimensions for our sensors eliminates uncertainties in optical responses compared to plasmonic devices thus grants the better sensing opportunities for future research work and making it a practical sensor (Vasquez 2016).

1.5 Aptamer Structural Design Changes

Aptamer is composed of short single stranded oligonucleotides (DNA/RNA/XNA (XenoNucleic Acid)), that binds to its respective target with high specificity and affinity via folding into tertiary structures (Ellington, 1990; Tuerk, 1990). Its' high binding affinity and specificity has created an interest over the traditional ELISA methods using antibodies, furthermore, has longer stability and flexibility in temperatures over the antibodies that a study recently has been developed to replace the antibodies with aptamers (Yildrim-Tirgil, 2022). As for dopamine aptamer, the original aptamer was extracted via in-vitro selection from a pool of RNA molecules that defined the binding mechanism of dopamine with the aptamers through tertiary binding between the 2 stems and loop motifs (Mannironi, 1997). It was further improved by converting this very RNA aptamer by converting

it into DNA aptamer, this essentially created a greater stability in binding due to the bonding in RNA essentially creates a domino effect where the binding isn't stable to shorting of the phosphate-to-phosphate bond and cause tertiary structural binding to be instable and the nucleotides responsible for binding of dopamine was maintained in the new DNA homolog (Walsh, 2009). This in return caused researcher to switch from RNA to DNA aptamers. Furthermore, this aptamer was improved by removing cross-reactive sequences via biotinylation and elution and improved the binding region due to its new capability of causing conformational changes when binding to dopamine thus create greater signal (Nakatsu, 2018). The evolution of the dopamine aptamer structural changes is reflected in figure 1 and further explanation is stated in the results & discussion section.

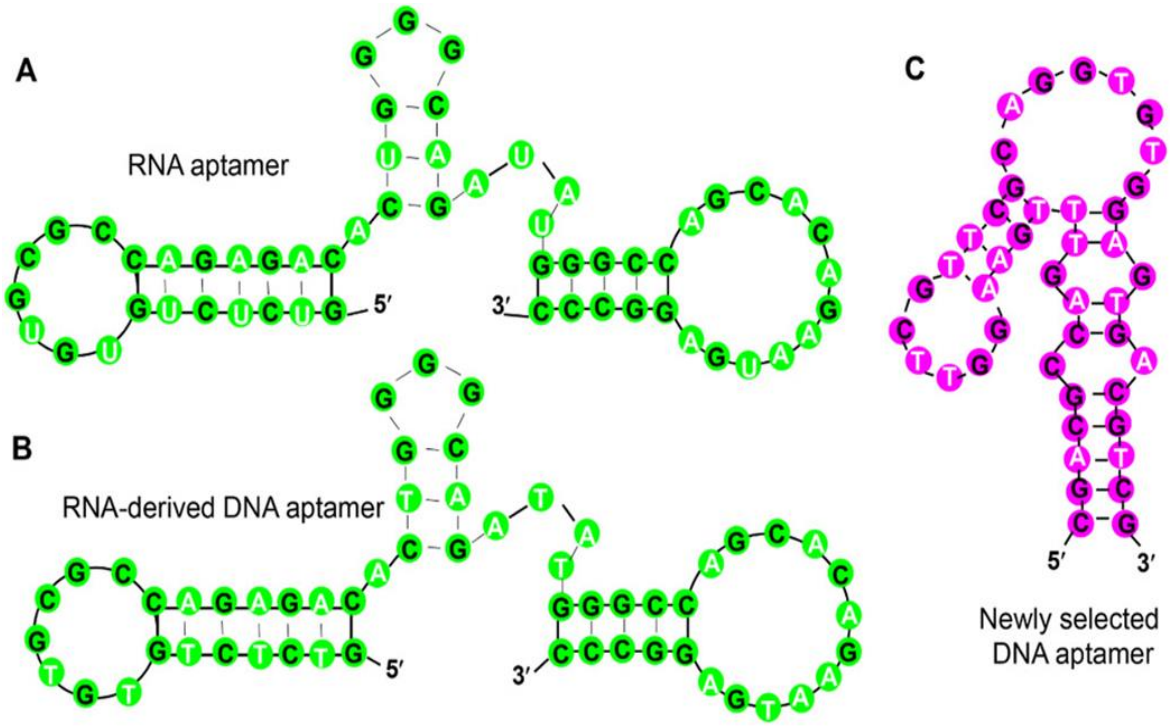

Figure 1: Dopamine aptamer structural changes

A) RNA aptamer extracted in 1997. B) The original DNA homolog dopamine aptamer converted from RNA aptamer in 2005. C) Newly selected aptamer that was developed in 2018 that is capable of structure switching when binding to dopamine. Reprinted with permission from "Dopamine and melamine binding to gold nanoparticles dominates their aptamer-based label-free colorimetric sensing" by Liu et al., 2020. Copyright 2020 American Chemical Society.

CHAPTER TWO: METHODS & MATERIALS

2.1 Fabrication of the plasmonic sensor

The fabrication of the sensor uses a standardized and known soft nanoimprint nanolithography technique. It requires clean glass slides that is cut into 1 inch by inch, which constitutes the base platform of the sensor. To prep the cut glass slides it must be submerged into acetone for 1 hour and sonicated. Then the glass slide requires to be cleaned in the respective order of acetone, isopropyl alcohol, and deionized water followed up with drying with nitrogen. A 5nm titanium adhesion layer is deposited on top of the glass and is followed up with 100 nm of gold is deposited on the glass/titanium substrate by electron-beam deposition. The substrate is then spin-coated with a negative photoresist (SU-8 2000.5, Kayaku Advanced Materials®) at 1750 rpm for 1 minute, followed by 1 minute of pre-baking of 95 degree celsius. This in turn forms the cavity for our sensor. It is then thermally embossed with a negative-pattern containing PDMS (poly dimethyl siloxane) nanoimprint stamp so as to transfer the hole-disk pattern on to the resist surface.

Furthermore, the substrate is exposed to UV light for 5 minutes to cure sample to cross-link the polymer and increase stability. A thin 20 nm layer of aluminum

oxide (Al2O3) is deposited using atomic layer deposition (ALD) on the substrate to create a passivation layer. Finally, 3 nm of Ti (titanium) adhesion layer is followed up with a 30 nm of Au is deposited by electron-beam deposition, which concludes the sensor fabrication process. Due to the ease and rapidness of the process, several sensors can be fabricated in one batch.

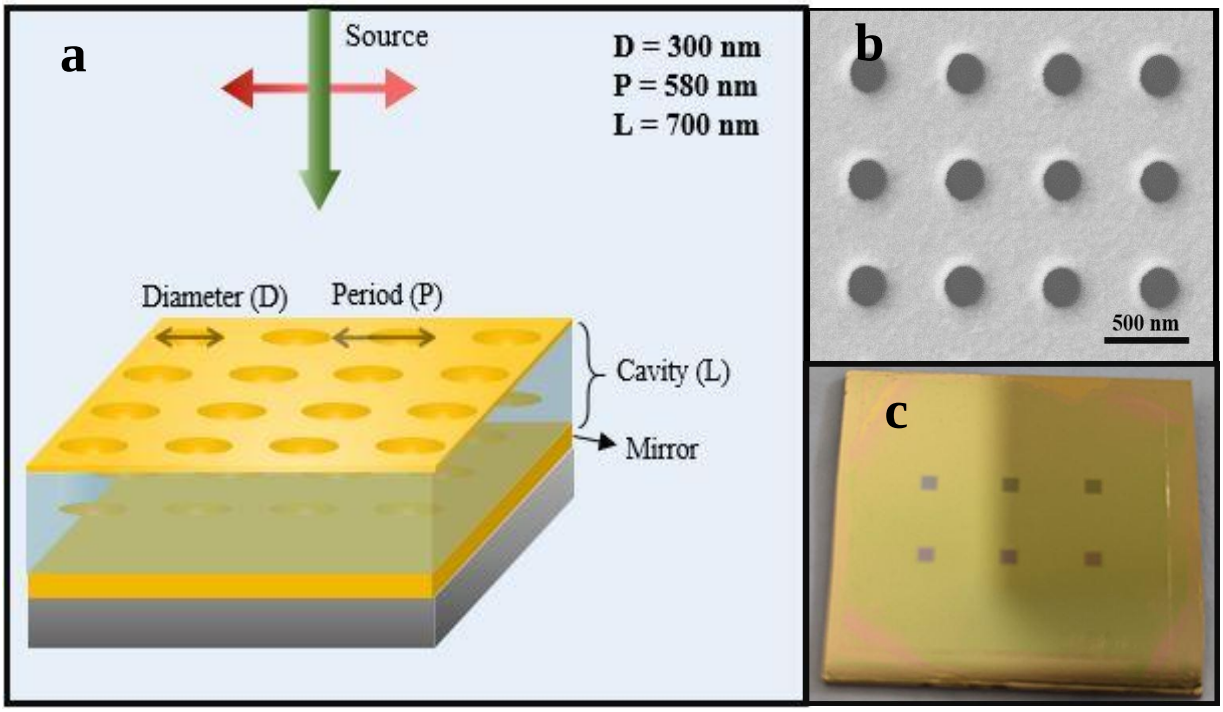

Figure 2: Sensor schematic

a) The Schematic representation of hybrid cavity-coupled plasmonic system in presence of diffraction. b) SEM image of the hole-disk pattern. c) Macroscopic image of the hybrid cavity-coupled plasmonic system used for biosensing. The respective periodicity, diameter, and length attributes to the spectral response wavelength.

2.2 PDMS baking and functionalization

Polydimethylsiloxane (PDMS) elastomer (Dow Corning Corporation) is mixed in 10:1 ratio to its curing agent, the mixed solution is vacuumed to be degassed and poured to 3 mm thick layer and is baked overnight at 75 degrees Celsius. The PDMS layer 6 x 3 mm holes are punched in to 20.4 mm by 12.7 mm to create a thin layer of wells to hold low volume solutions for the plasmonic sensors.

PDMS is baked for 45 minutes at 110 degrees Celsius, cool it down for 2 minutes. Plasma etch the PDMS for 5 minutes. Incubate polyvinyl alcohol (PVA) 5% w/v into each hole for 15 minutes. Clean with N2, then bake the sample on 110 degrees hotplate for 10 minutes.

2.3 Sensor Functionalization

The oligonucleotides were purchased from Integrated DNA technologies, Inc (Coraville, IA). The sequence of the aptamers are 5'-/ThioMC6D/ DGTC TCT GTG TGC GCC AGA GAC ACT GGG GCA GAT ATG GGC CAG CAC AGA ATG AGG CCC-3'(1997 DNA's analog) and 5'-/ThioMC6D/CGA CGC CAG TTT GAA GGT TCG TTC GCA GGT GTG GAG TGA CGT CG-3' (Nakatsuka, 2018). Upon

arrival the oligonucleotides were equilibrated in IDTE buffer (10 mM Tris, pH 8, 0.1 mM EDTA) was frozen as aliquots of 50 uL and stored at -20 ^{o}C. The folding buffer was made according as (137 mM Nacl, 10 mM Na_2HPO_4, 2.7 mM KCl, 2 mM $MgCl_2$, 1.8 mM KH_2PO_4, pH 7.4), and reducing buffer was made 20mM TCEP 20mM TCEP in Tris-Hcl buffer pH 7.4. The materials were purchased from Sigma Aldrich.

2.3.1 Aptamer preparation & Surface functionalization

The aptamer aliquot is thawed to room temperature, and 18uL of the aliquot and 2uL of folding buffer pipetted together to produce a concentration of 90uM. The mixture is then placed into a water bath for 5 min in 95 degrees Celsius. The mixture is then cooled for 15 minutes, and then mixed with reducing buffer (20mM of TCEP in Tris-HCl pH 7.4) 1:1 volume ratio for 15 min. The final concentration is 45uM. The final mixture is to be drop casted in the PDMS well for surface functionalization of the sensor.

The sensors were cleaned via rinsing in the respective order of acetone, isopropyl alcohol, and Deionized water following up with Nitrogen gas. Then the sensor placed on a hot plate for 3 minutes on 95 degrees Celsius. The sensor is then to be cooled to room temperature then plasma etched for 5 minutes followed by UV

treatment for 5 minutes. A hydrophilic PDMS functionalized via PVA, surface treatment dimensions are of 2 mm thick with six holes where each diameter of 3mm wide was placed on top of each sensor (Vasquez-guardado, 2021). Each hole contains 6uL of aptamer mixture and were incubated for 4 hours in a petri dish that was sealed with parafilm and placed on a shaker at 200 rpm. Rinsed with DI water and dried with nitrogen gas, followed up with incubating 6uL of 6-mercapto-hexanol (MCH) (Sigma-Aldrich, St. Louis, MO) for 1 hour in a cool dark place sealed in a petri dish with parafilm. After this incubation step, it was then rinsed with DI water and nitrogen gas, and it is then ready to be introduced with the respective analytes and interfering species.

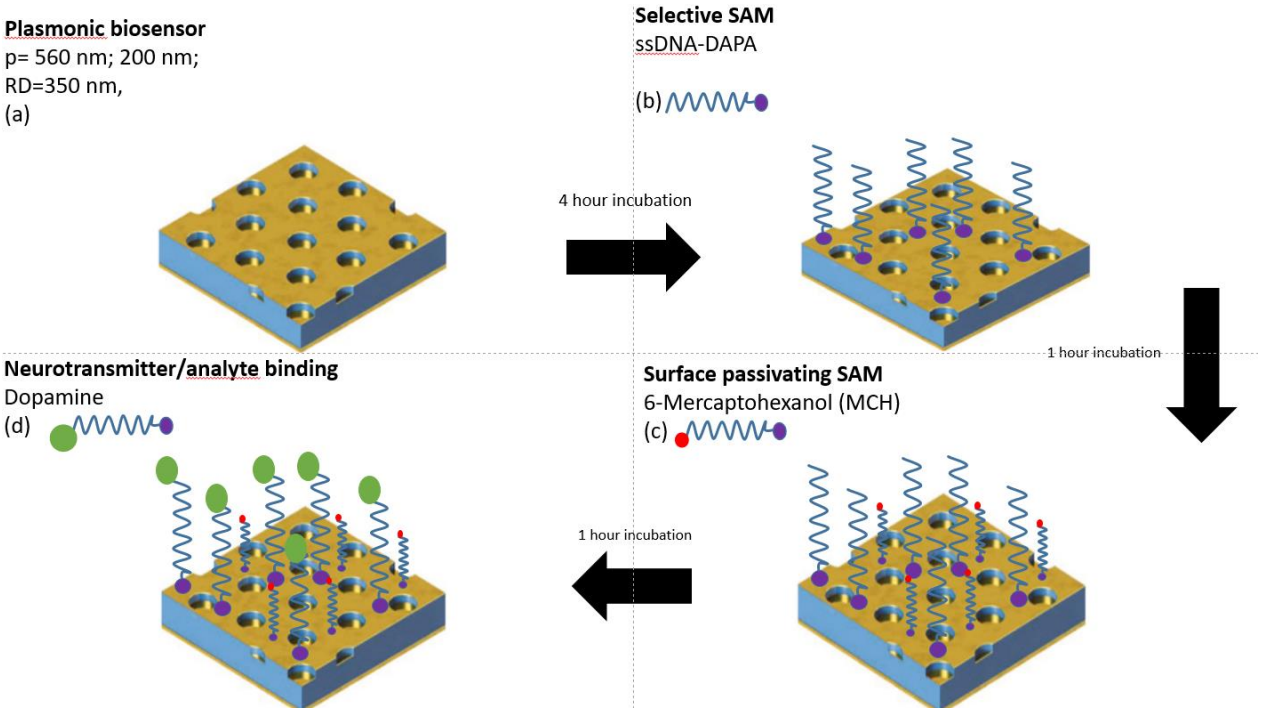

Figure 3: Workflow schematic

(a) The sensors were cleaned with acetone, IPA, and DI water followed by plasma etching and UV treatment. (b) thiol-terminated on 5' end of the ssDNA aptamer specific to dopamine binding is activated with TCEP prior to incubation on the sensor for 4 hours (c) 6-mercaptohexanol (MCH) is a self-assembled monolayer that is incubated onto the sensor for 1 hour to block the remaining spots and is bound to the surface via covalent bonds, this is to decrease biofouling and nonspecific binding. (d) Dopamine is incubated onto the sensor for 1 hour and LSPR shift is recorded thereafter.

2.4 Instruments and Analysis

The optical set up as demonstrated in Figure 4 is used to measure the plasmonic sensors uses tungsten light source, that is used to illuminate for imaging and reflection spectroscopy, coupled to a 100 µm core diameter optical fiber cable. The light will go through the lens to hit the 50:50 beam splitter and direct towards the sample and back. The reflected light after hitting the 50:50 beam will then hit the 10:90 beam splitter and direct 90 percent of the reflected light to the Vis-NIR spectrometer (HR2000+, Ocean Optics/Ocean Insight) via 400 µm core diameter optic fiber. The remaining 10 percent is used to illuminate and create an image of the surface of the sample. This feature is used in conjunction with Labview Interface and OceanView software to direct the light source for measurements by moving the platform in X/Y/Z axis towards desired location of the sample.

The OceanView Software is a software that provides but not limited to real-time control and processing of the measurements given in a visual graph of absorbance spectrum and reflectivity. The OceanView Software was used to process the recording of the different stage's incubation of the sample throughout the research. In this research, the reflectivity vs wavelength mode was selected to record our data analysis. Before each use, the software must be calibrated to an average of

10 scans and box car with of 5 to initially configure the visual setting of the analytical tool. To set the reflectance parameters of total reflectivity, a gold mirror was used and placed below the spectrometer. The built-in camera from the optical setup was used as a guideline to fine tune the platform to the spectrometer readings. For total non-reflectivity or absence of light, the black matted box was placed under the spectrometer and with the given light from the spectrometer being absorbed sets the final configuration for the spectrometer and the OceanView software. The spectrometer will used take the reading in of transmittance, absorbance, and reflectivity to create spectral responses of the respective sample's surface.

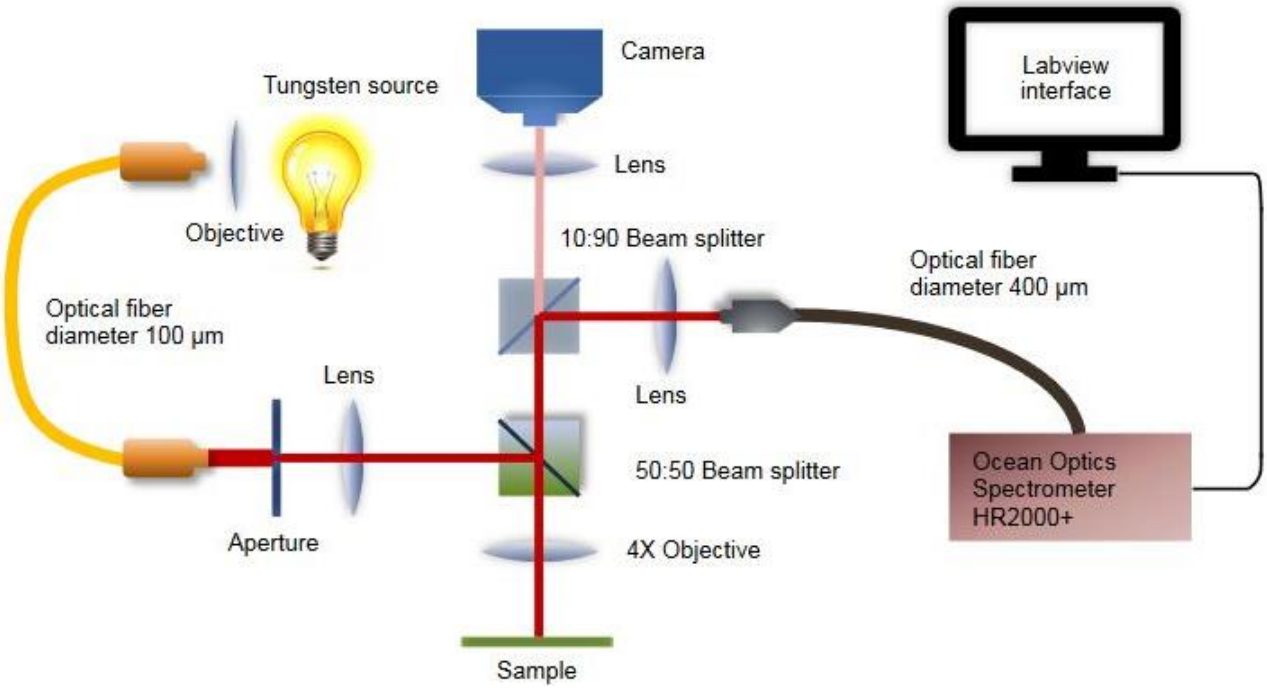

Figure 4: Optical setup using reflectance spectroscopy

This figure represents the optical setup employed for measuring the sensors. The reflection eventually is reflected into the ocean optics spectrometer and processed by the OceanView Software to display spectral peaks of the sample's respective surface area. Reprinted with permission from "Enzyme-Free Plasmonic Biosensor for Direct Detection of Neurotransmitter Dopamine from Whole Blood," Vasquez-Guardado (2019), Copyright 2019 American Chemical Society.

2.4.1 Aptamer Incubation and Dopamine Binding Analysis

The spectral LSPR response from the sample is collected from the OceanView software is fitted with a Guassian function in MATLAB to accurately determine the LSPR peak absorption wavelength's minima. The spectral shift is determined by difference of the final and initial measurement. For example, if the MCH is the (λ_0) initial measurement then the (λ_f) final measurement would be the dopamine incubation thus the spectral shift or the difference of the final and initial measurement be simply summed up as $\Delta\lambda = \lambda_f - \lambda_0$ and is demonstrated in figure 5a. The spectral differences between the incubation of dopamine and MCH is the main point of reference to determine the binding affinity of dopamine aptamer.

The sensor was measured different stages of the experiment when it was bare, post aptamer functionalization, post MCH incubation, and then incubation of dopamine and other analytes as demonstrated in Figure 5b. Each stage was cleaned with DI water and dried with nitrogen before measurement to ensure no excess constituents remained.

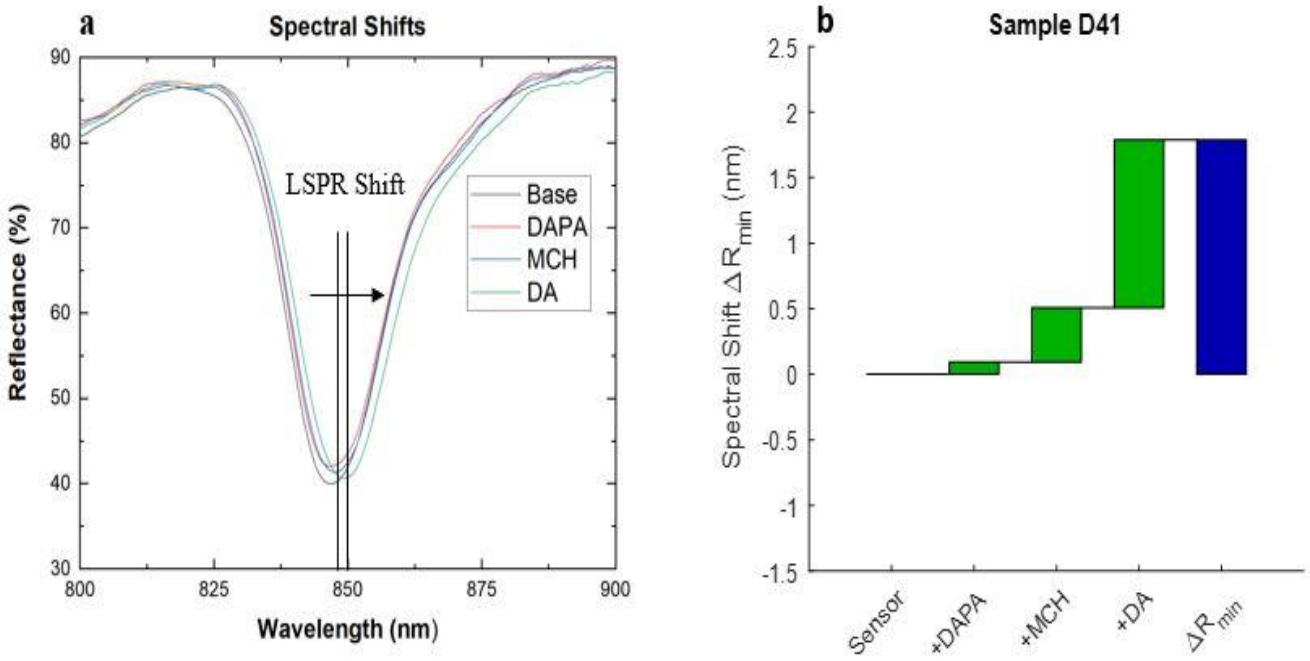

Figure 5:Spectral Shift and Waterfall chart

a) LSPR shift is determined by the difference of the DA and MCH spectral peak wavelength position. b) The Waterfall chart is a chart used to reflect spectral shifts between each incubation point of the experiment.

2.5 AFM imaging

Atomic force microscopy (AFM) images were taken via tapping mode using silicone tips (Neaspec) to characterize the polymer layer on the gold surface area. A gold mirror (100 nm Au on glass slide) was used as a platform to incubate thiolated dopamine aptamer, MCH, and dopamine in the respective order as mentioned in aptamer preparation and surface functionalization protocols. The respective organic compounds were incubated in the respective order, and each step was measured multiple times in the surface area 2.8 μm x 2.8 μm parameter via tapping mode in 285 kHz and to obtain root mean square (RMS) roughness of the respective surface area of interest and height (Jarczewska, 2018; Jolly, 2016).

CHAPTER THREE: RESULTS AND DISCUSSION

3.1 Results

3.1.1 AFM studies on dopamine aptamer layer

AFM imaging was used to determine thiolated dopamine's attachment to the gold surface as well dopamine binding to aptamer. Surface roughness and height was extracted from the topography of the measured sample via AFM. As shown in figure 6, The root mean square (RMS) roughness of the gold surface was 1.5 nm, and this increased to 1.7 nm with the following formation of DA aptamer with MCH. The following's height increased from 13 nm to 37 nm as indicated in figure 6a and 6b post incubation of aptamers and MCH. The roughness increased 1.7 nm to 16.4 nm and height 37 nm to 101 nm post DA incubation to the thiolated DA aptamer with self-assembled monolayer MCH. With the removal of excess unbound aptamer and MCH monolayer with DI water rinsing and nitrogen gas and MCH's blocking the remaining surfaces, to prevent indirect dopamine's tendency to bind to the gold surface, narrows the margin of error and ensures that there is actual binding

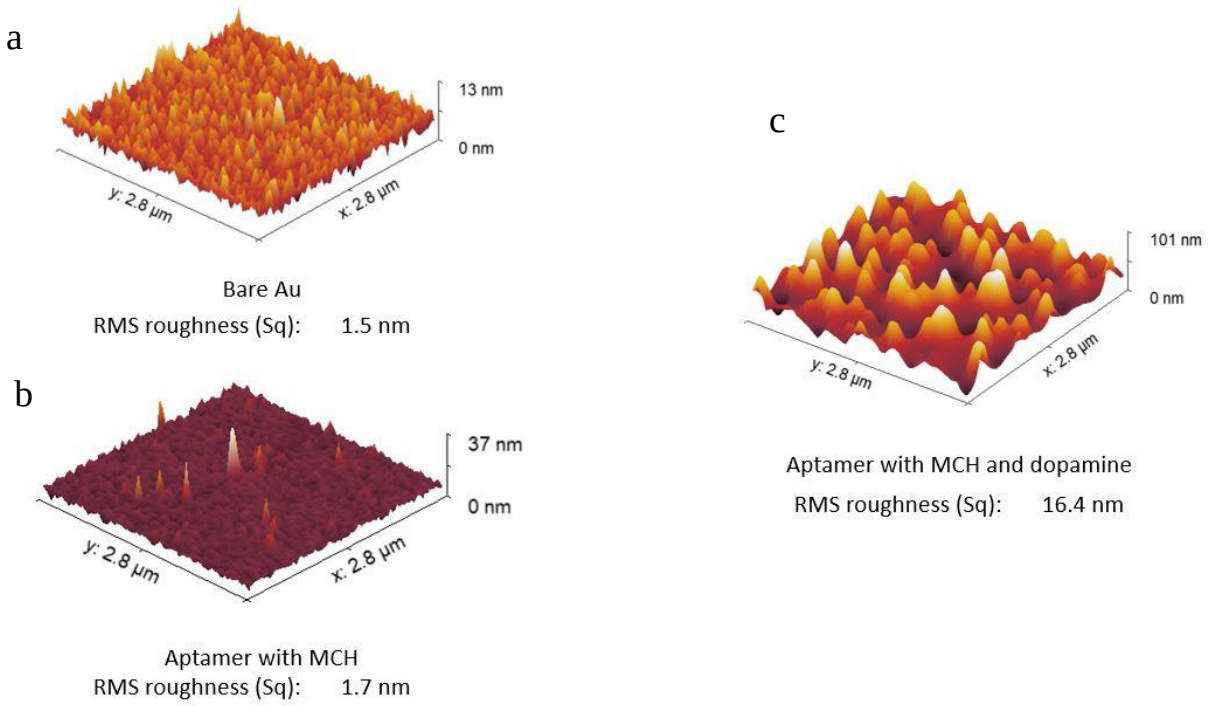

Figure 6: Surface roughness measurement by AFM

The surface roughness and height of each incubation process. The surface roughness and height demonstrate the presence thiolated aptamer and successful binding of dopamine. a) Bare Gold, b) aptamer & MCH, c) aptamer & MCH with dopamine

3.1.2 Comparison of Aptamers

The 2 aptamers that are to be compared is the DNA dopamine aptamer that was converted from the RNA dopamine Aptamer that we will call 57mer and the newly synthesized ssDNA dopamine aptamer in 2020 as 44mer (Walsh, 2009). We compared the 2 aptamers binding potential to dopamine and its correlation in respect to the concentration, both followed the standard operating procedure and measured the reflectivity of the sensor surface in each incubation process. Each solution such as 6-mercaptohexanol, dopamine aptamer mix solution, and dopamine in PBS's volume were in low volume. In figure 7 as shown below shows the spectral shift of the sensor in respects to surface reflectivity from MCH incubation.

As literature states, the original DNA converted aptamer homolog 57mer doesn't have great binding and is reported to not bind specifically (Hou 2021), whereas an electrochemistry study claimed that 57mer cannot bind to dopamine (Alvarez-Martos, 2017). From the comparison between 57mer and 44mer is dopamine binding in contrast to LSPR shift, it can be stated that the 57mer does bind to dopamine, but does not have a consistent LSPR shift as noted by the large standard deviation in the error bars in figure 7. This can be hypothesized that it doesn't directly bind to dopamine and agree with other literature. In comparison for 44mer, it has shown greater and consistent binding of dopamine as reflected by the LSPR

shift and the standard deviation from figure 7. We conclude that with the given trend from low to high concentration of dopamine is consistent comparing to 57mer supports the theory that 44mer directly binds to dopamine whereas 57mer does not. The LSPR shift also is greater thus trend from the high to low concentration of dopamine as reflected by the LSPR shift from figure 7. Furthermore, it can be stated that the error bars span to negative values for 57mer in lower concentration due to huge variance in the spectral shifts and sometimes not even binding to dopamine at the lower concentration and cause negative or blue shifts, which can only conclude that the 57mer isn't reliable for dopamine binding. In contrast, 44mer was able to consistently red shift from post incubation of dopamine thus indicates reliability of the new aptamer.

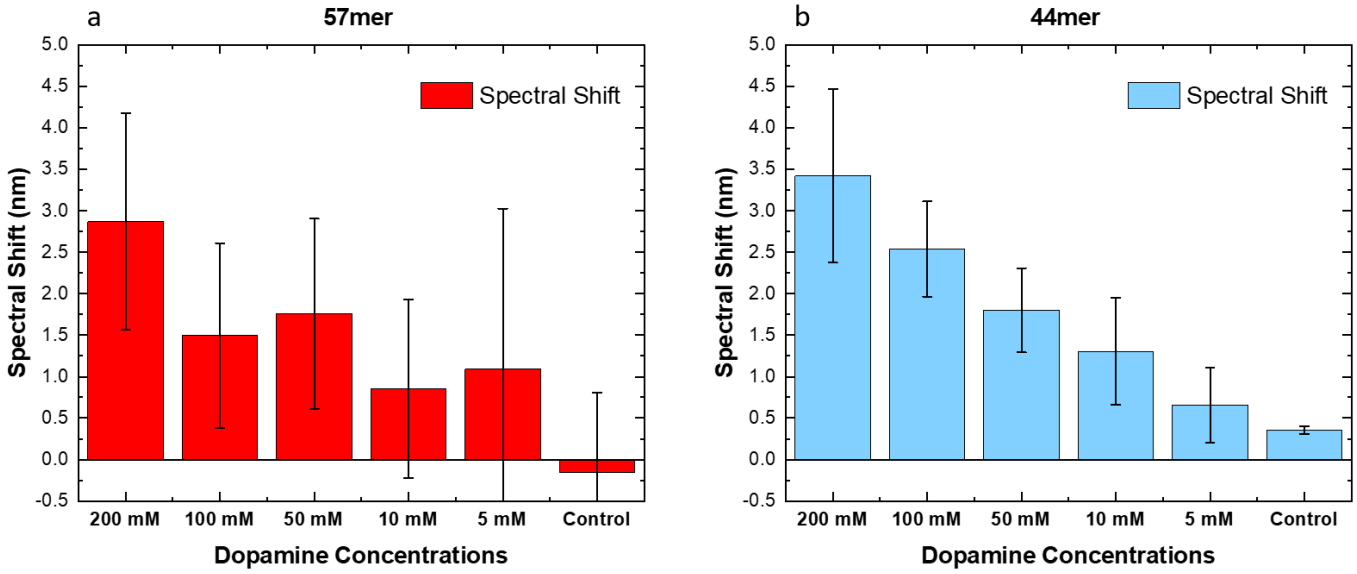

Figure 7: Spectral Shift of 57mer vs 44mer

Spectral shift in reflection was measured from concentrations of 200mM, 100mM, 50mM, 10mM, 5mM and PBS as control. a) 57mer is a DNA homolog DA aptamer created by Walsh (2009) b) 44 aptamer is the DA aptamer created by Nakatsu (2018). The spectral shift and standard deviation of each aptamer in respect to concentrations of dopamine demonstrates the binding and its' affinity to dopamine. Uncertainty bars represent standard deviation (S.D.)

3.1.3 Specificity of the aptamer binding in the interfering species

In blood and in CSF there are other metabolites and precursors of dopamine that can be found within said solution. To ensure that the aptamer does not bind to other constituents or cause false readings, an experiment was carried out to determine that the aptamers are specifically binding to dopamine, different metabolites and precursors of the dopamine aptamer was introduced to view comparison. Such lists include Homovanillic Acid (HVA), epinephrine(EPI), Levodopa (L-Dopa) as well as PBS for control. As shown in figure 8, 100 mM as well as 10 mM of dopamine was tested alongside with the other interfering species to show consistency of the spectral shift. The interfering species when compared to dopamine in the same concentration has shown no binding to the dopamine aptamer. The lack of binding is represented by the negative or red shift in reflectivity.

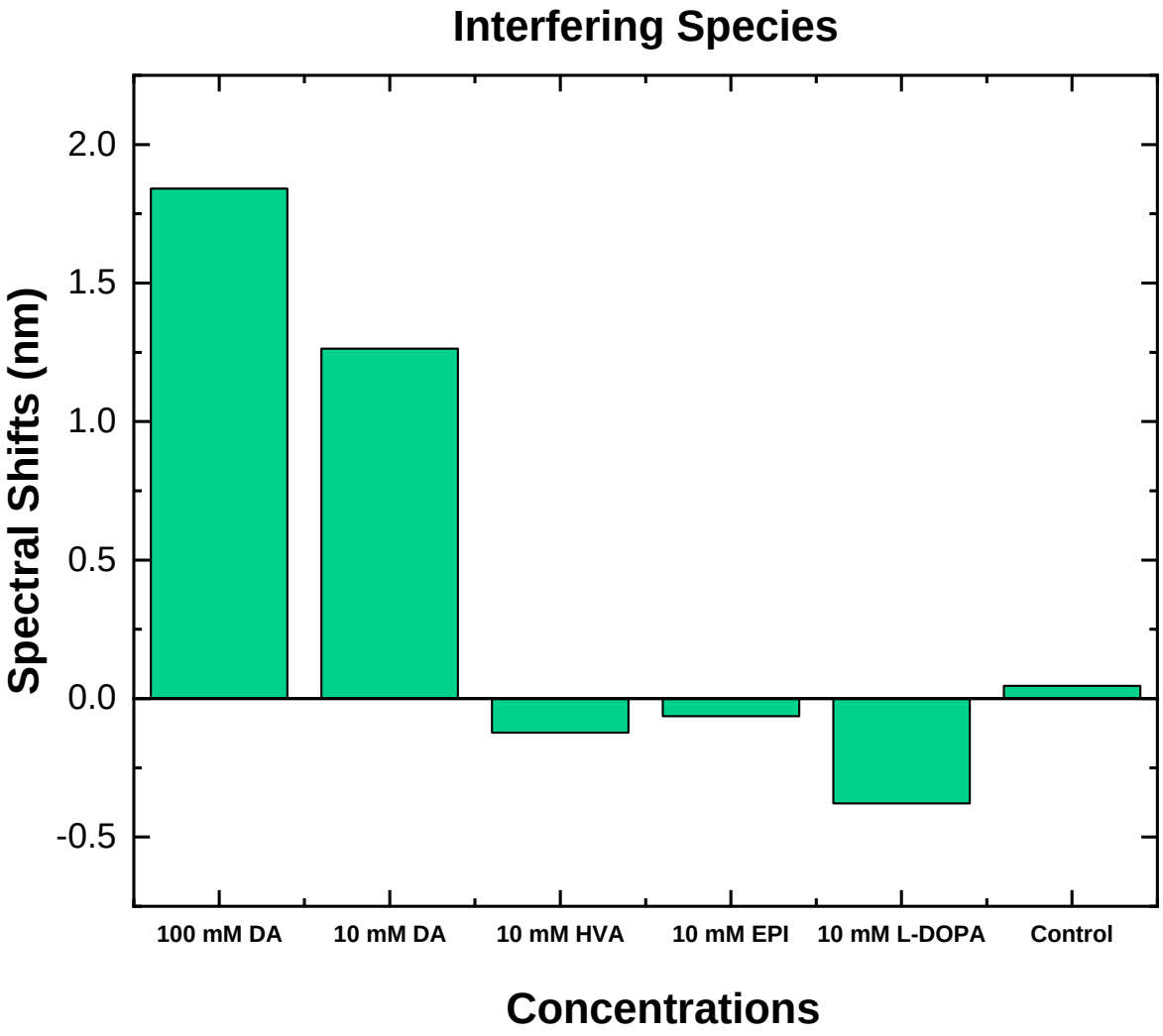

Figure 8: Interfering species

Spectral shifts of dopamine and other metabolites and precursors of dopamine such as Homovanillic acid (HVA), Epinephrine (EPI), and Levodopa (L-DOPA) along with PBS as control.

3.1.2 Limits of Detection of the plasmonic sensors in the drop cast method

To see the lowest concentration the plasmonic sensors can detect using low volume of dopamine, lower concentrations of dopamine was introduced while using 10mM as the baseline from the previous measurement for comparison. It is currently hypothesized that with the given volume 6uL of 5 mM of dopamine is the current limit that the plasmonic sensor can detect with the drop cast method as shown in figure 9. This is due to the fact that we believe that any spectral shift from 0.5nm and below can be considered noise despite some trend showing.

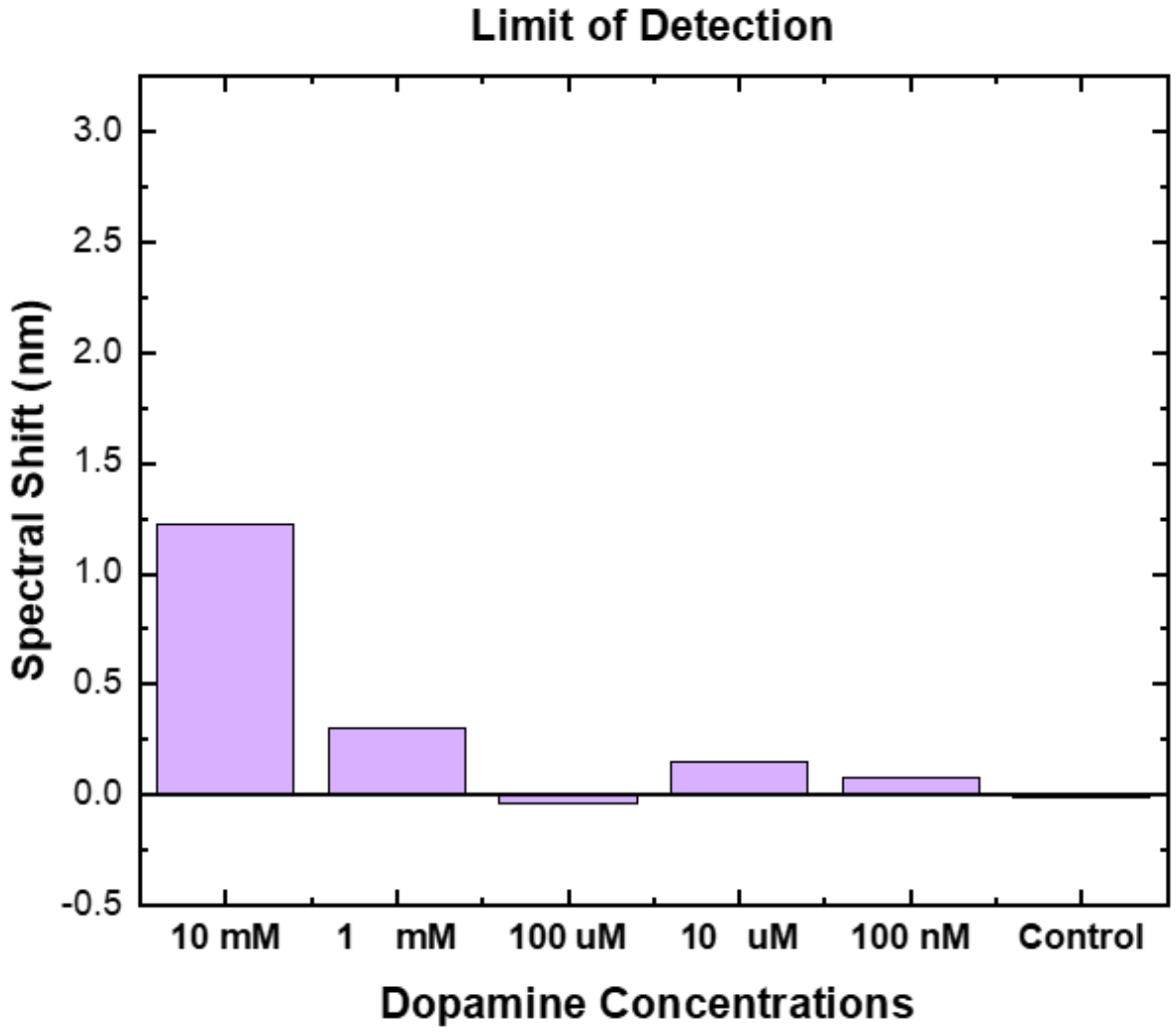

Figure 9:Limit of detection

This graph shows the change of the change of spectral shifts in the reflection from concentrations of 10mM, 1mM, 10uM, 100nM, and PBS as control.

3.2 Discussion

DNA and RNA have similar structure, but due to their unique nucleotide such thymine and uracil it as well as 2' hydroxyl in RNA specifically contributes to the tertiary structural change and stability (Walsh, 2009). Predominately the 2' hydroxyl group of the RNA forces the ribose that reads into a 3'-endo pucker where it will produce a significantly shorter phosphate-phosphate distance in the backbone thus creating a more compact helical conformation compared to DNA's B-form. This in return changes the structure a greater amount for it causes a chain reaction by changing major, minor grove width, twist angle and axial diameter for the end product (Walsh, 2009). Therefore, it was concluded that DNA version of the aptamer is much more stable, and was concluded that the binding domain for dopamine remained intact with an high affinity (K_d 0.7uM) based on fluorescence anisotropy(Walsh, 2009).

The binding domain of the DNA homolog of the RNA Aptamer is highly dependent on Watson and Crick base pairing and was concluded that the 5 nucleotides responsible for dopamine binding is "G13, C14, A41, G51,G52" (Walsh, 2009). The newly synthesized aptamer were created by attaching the oligonucleotide library agarose-streptavidin columns through biotinylation, was eluted, and removed cross-reactive sequences of the aptamer. This in return caused the newly designed

aptamer to produce a stronger signal compared to Walsh's study and the process caused the aptamer's recognition/binding region (isolated aptameric stem-loop receptors) to be capable of conformational changes (Nakatsu, 2018). Using the same aptamer, another group reported a K_d of 1.9 uM using isothermal titration calorimetry despite using structure-switching selection method had produced excellent binding and little to no binding to interfering species with AuNP (Liu, 2020; Hou, 2021).

The practical implementations of the plasmonic sensor functionalized with DNA aptamer is that it creates a fine-tuned detector with high specificity geared towards the specific analyte it is trying to detect. We believe that this platform can be useful as an early diagnosis for neurological diseases such as PD, ADHD, and Alzheimer's etc. Furthermore, Cerebral spinal fluids collection is an invasive and expensive procedure, with this current dopamine detection sensor requiring ultra-low volume there may be some practical use in this scenario. The current challenge with this platform is that the incubation of the aptamer is from drop cast method, it can be improved with pre-functionalized alkanethiols to reduce steric hinderance which has been currently developed but requires additional time to carry out. Another challenge for this current method is that the process is labor intensive and is very time restrictive from each stage of the incubation. It can be suggested that

3.3 Future Work

The vision for the future works of the plasmonic sensor functionalized with aptamer is to create a convenient, low cost, and label free dopamine detection for clinical care or for home use as a point of care system. The current plasmonic sensor will detect from dopamine plasma like fluids without any preparation or reagents, but we are hoping to take this platform to the next step by being able to detect dopamine in blood and other biologically relevant fluids.

Furthermore, the sensors can be functionalized with other aptamers that are specifically designed for other neurotransmitters so it can detect multiple neurotransmitters from the same biological fluids. We have in the past have demonstrated real time sensing of other substrates such as dengue virus with a microfluidic plasma separator made up of PDMS. And other compounds such that isn't organic such as inorganic amine-coated iron oxide nanoparticles. With this same concept, we can introduce other analytes.

APPENDIX A

COPYRIGHT PERMISSION

APPENDIX B
DEFENCE ANNOUNCEMENT

Announcing the Final Examination of Sang Lee for the degree of Master of

Science in Nanotechnology

Date: Tuesday, November 15th, 2022
Time: 4:30 PM EST
Room: Virtual (Zoom)

Link:https://ucf.zoom.us/j/97078707012?pwd=c0dhQ1NZeHhZeEhDZk1BQmtWb0hFQT09

Meeting ID: 970 7870 7012
Passcode: 295387

Thesis Title: **Plasmonic Sensor based Detection of Dopamine**

Abstract

With a rapidly ageing population, neurological diseases are becoming increasingly relevant in the design of public health policies and strategies in western societies. In the last decades, biochemical research has consistently shown the critical role that neurotransmitters and their associated metabolites play as biomarkers in tracking and diagnosis of different brain disorders and cancers. In particular, dopamine, an organic electrochemical neurotransmitter, has been shown to be paramount for the proper functioning of the neural system. Dopamine's dysfunction, has been shown to underlie the pathogenesis in several neurological disorders such as Parkinson's disease, depression, chronic schizophrenia and psychosis. Unfortunately, currently available diagnostic technologies require expensive equipment and trained personnel, thus slowing the process and increasing overall costs, consequently reducing the access to the general population. Ideal sensing alternatives should offer low-cost, fast, and reliable point-of-care diagnosis. In this work, we present a compact label-free plasmonic biosensors that exhibits sharp optical resonance shifts in response to varying dopamine concentrations. While the nanoimprinting of the optical cavity offers a nanofabrication process fully compatible with large-scale production, its small size ensures the suitability for integration on lab-on-a-chip platforms, hence making it a promising alternative to conventional diagnosis. The plasmonic nanostructures of the chips are functionalized with synthetic single-stranded oligonucleotide to

ensure precise sensing selectivity. Particularly, we study the standard 57mer and the novel 44mer configurations, establishing the superior resolution offered by the latter. In contrast to other sensing alternatives, our platforms permit reliable detection with ultralow volumes (~6 L) and exhibit robustness to interfering species. This work paves the way towards the first generation of low-cost, ultra-low volume, on-chip sensors for in-situ tracking of dopamine.

Thesis Committee:
Dr. Debashis Chanda (Chair)
Dr. Ellen Kang
Dr. Kiminobu Sugaya
Dr. Sudipta Seal

Approved for distribution by Dr. Debashis Chanda, Committee Chair, on November 1st, 2022

REFERENCES

Adams, R. (1990). In vivo electrochemical measurements in the CNS. *Progress in Neurobiology, 35*(4), 297-311. doi:10.1016/0301-0082(90)90014-8

Anagnoste, B., Freedman, L. S., Goldstein, M., Broome, J., & Fuxe, K. (1972). Dopamine-β-hydroxylase activity in mouse neuroblastoma tumors and in cell cultures. *Proceedings of the National Academy of Sciences, 69*(7), 1883-1886. doi:10.1073/pnas.69.7.1883

Dubois, L. A., & Gray, D. K. (2005). Dopamine-secreting pheochromocytomas: In search of a syndrome. *World Journal of Surgery, 29*(7), 909-913. doi:10.1007/s00268-005-7860-7

Ellington, A. D., & Szostak, J. W. (1990). In vitro selection of RNA molecules that bind specific ligands. Nature, 346(6287), 818–822. https://doi.org/10.1038/346818a0

Fuxe, K., Borroto-Escuela, D. O., Romero-Fernandez, W., Zhang, W., & Agnati, L. F. (2013). Volume transmission and its different forms in the central nervous system. *Chinese Journal of Integrative Medicine, 19*(5), 323-329. doi:10.1007/s11655-013-1455-1

Hou, Y., Hou, J., & Liu, X. (2021). Comparison of two DNA aptamers for dopamine using homogeneous binding assays. *ChemBioChem, 22*(11), 1948-1954. doi:10.1002/

Jarczewska, M., Rębiś, J., Górski, Ł., & Malinowska, E. (2018). Development of DNA aptamer-based sensor for electrochemical detection of C-reactive protein. Talanta, 189, 45–54. https://doi.org/10.1016/j.talanta.2018.06.035 bic.202100006

Jolly, P., Tamboli, V., Harniman, R. L., Estrela, P., Allender, C. J., & Bowen, J. L. (2016). Aptamer–MIP hybrid receptor for highly sensitive electrochemical detection of prostate specific antigen. Biosensors and Bioelectronics, 75, 188–195. https://doi.org/10.1016/j.bios.2015.08.043

Lakard, B. (2020). Electrochemical biosensors based on conducting polymers: A Review. *Applied Sciences, 10*(18), 6614. doi:10.3390/app10186614

Liu, X., He, F., Zhang, F., Zhang, Z., Huang, Z., & Liu, J. (2020). Dopamine and melamine binding to gold nanoparticles dominates their aptamer-based label-free colorimetric sensing. *Analytical Chemistry, 92*(13), 9370-9378. doi:10.1021/acs.analchem.0c01773

Mannironi, C., Di Nardo, A., Fruscoloni, P., & Tocchini-Valentini, G. P. (1997). in vitro selection of dopamine RNA ligands. Biochemistry, 36(32), 9726–9734. https://doi.org/10.1021/bi9700633

Mattson, M. P., & Magnus, T. (2006). Ageing and neuronal vulnerability. *Nature Reviews Neuroscience, 7*(4), 278-294. doi:10.1038/nrn1886

Nakatsuka, N. (2019). Faculty opinions recommendation of aptamer-field-effect transistors overcome Debye length limitations for small-molecule sensing. *Faculty Opinions – Post-Publication Peer Review of the Biomedical Literature*. doi:10.3410/f.733951059.793567197

Nemiroski, A., Gonidec, M., Fox, J. M., Jean-Remy, P., Turnage, E., & Whitesides, G. M. (2014). Engineering shadows to fabricate optical metasurfaces. ACS Nano, 8(11), 11061-11070. doi:10.1021/nn504214b

Pagano, G., Ferrara, N., Brooks, D., & Pavese, N. (2016, April 12). Age at onset and parkinson diseasephenotype.RetrievedOctober28,2022,from https://www.ncbi.nlm.nih.gov/pmc/articles/PMC4831034/

Robinson, D. L., Hermans, A., Seipel, A. T., & Wightman, R. M. (2008). Monitoring Rapid Chemical Communication in the brain. *Chemical Reviews, 108*(7), 2554-2584. doi:10.1021/cr068081q

Ruffolo, R. R., Messick, K., & Horng, J. S. (1984). Interactions of three inotropic agents, ASL-7022, dobutamine and dopamine, with α- and β-adrenoceptors in vitro. *Naunyn-Schmiedeberg's Archives of Pharmacology, 326*(4), 317-326. doi:10.1007/bf00501436

Schultz, S., Smith, D. R., Mock, J. J., & Schultz, D. A. (2000). Single-target molecule detection with nonbleaching multicolor optical immunolabels. Proceedings of the National Academy of Sciences, 97(3), 996-1001. doi:10.1073/pnas.97.3.996

Stoessl, A. J. (2012). Neuroimaging in parkinson's disease: From pathology to diagnosis. *Parkinsonism & Related Disorders, 18*. doi:10.1016/s1353-8020(11)70019-0

TIPPETT, P. A., McEWAN, A. J., & ACKERY, D. M. (1986). A re-evaluation of dopamine excretion in phaeochromocytoma. *Clinical Endocrinology, 25*(4), 401-410. doi:10.1111/j.1365-2265.1986.tb01706.x

Tuerk, C., & Gold, L. (1990). Systematic evolution of ligands by exponential enrichment: RNA ligands to bacteriophage T4 DNA polymerase. Science, 249(4968), 505–510. https://doi.org/10.1126/science.2200121

Vázquez-Guardado, A., Chanda, D., Seal, S., Das, S., Dennis, W., Biswas, A., . . . Barkam, S. (2019). Enzyme-free plasmonic biosensor for direct detection of neurotransmitter dopamine from whole blood. *Nano Letters*. doi:10.1021/acs.nanolett.8b04253.s001

Vázquez-Guardado, A., Smith, A., Wilson, W., Ortega, J., Perez, J. M., & Chanda, D. (2016). Hybrid cavity-coupled plasmonic biosensors for low concentration, label-free and selective biomolecular detection. *Optics Express, 24*(22), 25785. doi:10.1364/oe.24.025785

Vázquez-Guardado, A., Smith, A., Wilson, W., Ortega, J., Perez, J. M., & Chanda, D. (2016). Hybrid cavity-coupled plasmonic biosensors for low concentration, label-free and selective biomolecular detection. *Optics Express, 24*(22), 25785. doi:10.1364/oe.24.025785

Walsh, R., & DeRosa, M. C. (2009). Retention of function in the DNA homolog of the RNA dopamine aptamer. *Biochemical and Biophysical Research Communications, 388*(4), 732-735. doi:10.1016/j.bbrc.2009.08.084

Wightman, R. M. (1981). Microvoltammetric electrodes. *Analytical Chemistry*, *53*(9). doi:10.1021/ac00232a004

Wild, D. G. (2007). *The immunoassay handbook*. Amsterdam: Elsevier.

Yang, W., Hamilton, J. L., Kopil, C., Beck, J. C., Tanner, C. M., Albin, R. L., . . . Thompson, T. (2020). Current and projected future economic burden of parkinson's disease in the U.S. *Npj Parkinson's Disease*, *6*(1). doi:10.1038/s41531-020-0117-1

Yi, J. W., Oh, E. M., Lee, K. E., Choi, J. Y., Koo, D. H., Kim, K. J., . . . Youn, Y. (2012). An exclusively dopamine secreting paraganglioma in the retroperitoneum: A first clinical case in Korea. *Journalof the Korean Surgical Society*, *82*(6), 389. doi:10.4174/jkss.2012.82.6.389

Yildirim-Tirgil, N. (2022). Development of aptamer-based elisa method for d-dimer detection. Biotechnology and Applied Biochemistry. https://doi.org/10.1002/bab.2347